Journal of Machine Engineering, 2019, Vol. 19, No. 1, 71–85
ISSN 1895-7595 (Print) ISSN 2391-8071 (Online)

Received: *19 September 2018* / Accepted: *09 February 2019* / Published online: *11 March 2019*

polishing, linear motor,
mirror-like surface,
high quality

Ikuo TANABE[1*]
Valerio DE SOUSA GAMA[2]
Yoshifumi ISE[2]
Satoshi TAKAHASHI[1]
Hiromi ISOBE[1]

DEVELOPMENT OF A HIGH-SPEED MIRROR-LIKE FINISH POLISHING TECHNOLOGY FOR MINUTE PARTS BASED ON A LINEAR MOTOR

As high speed, high acceleration and stable drive on machine tools is constantly growing in demand, the use of linear motors in machine tools has increased. On the other hand, in order to achieve a high degree of quality, the need for mirror-like finish surfaces on industrial products has also considerably increased. This research explores the use of linear motors to develop a high-speed fine polishing process that achieves a mirror-like finish surface on small parts. The first stage of this process consisted in developing a polishing device, which was composed of a NC milling machine, a linear motor drive and a polishing head. Specifically, a polishing head attached to a linear motor drive was coupled with the spindle of a NC milling machine. A substitute for a small linear motor drive was obtained from a commercially available shaver, while the polishing head was made of propylene. The polishing head elaboration process, linear motor drive properties, lapping agent and the optimum polishing conditions were investigated in several experiments. The evaluation consisted in the high-speed polishing of minute areas on flat surfaces using the selected optimum conditions. It is concluded that, (1) the proposed system was able to achieve a mirror-like finish surface, (2) when compared to polishing with an ultrasonic motor, the machining time of the proposed system was reduced by half, (3) the proposed system was able to achieve a mirror-like finish on a 3 mm square sided area.

1. INTRODUCTION

As high speed, high acceleration and stable drive on machine tools is constantly growing in demand, the use of linear motors in machine tools has increased [1, 2]. Linear motors offer a high-speed feed, high acceleration and deceleration characteristics, along with a low vibration drive (when compared to a ball screw drive). On the other hand, the need for mirror-like finish surfaces on industrial products has also considerably

[1] Nagaoka University of Technology, Department of Mechanical Engineering, Niigata, Japan
[2] Nagaoka University of Technology, Graduate School of Mechanical Engineering, Niigata, Japan
[*] E-mail: tanabe@mech.nagaokaut.ac.jp
https://doi.org/10.5604/01.3001.0013.0454

increased [3]. Thus, amidst the demand for high-speed machine tools and processes, the need for high-speed polishing and automatic polishing technologies was highlighted [4]. This research explores and evaluates the usage of a small linear motor to develop a high-speed fine polishing automatic process that achieves a mirror-like finish surface on small flat parts. The first stage of this process consisted in developing a polishing device, which was composed of a NC milling machine, a linear motor drive and a polishing head. Specifically, a polishing head was attached to a linear motor drive. A substitute for a small linear motor drive was obtained from a commercially available shaver, while the polishing head was made of propylene. The polishing head elaboration process, linear motor drive properties, lapping agent and the optimum polishing conditions were investigated in several experiments. Subsequently, the evaluation of this system was based on the high-speed polishing of minute areas on flat surfaces using the selected optimum conditions.

A commercially available shaver was selected to function as a linear motor drive because these machines can achieve significantly high speed and precision at low cost. Here, the polishing of small flat parts was thought to be possible as the selected linear motor drive can function with batteries and achieves a small amplitude of 1 mm.

2. DEVELOPMENT OF HIGH-SPEED POLISHING PROCESS TECHNOLOGY USING A LINEAR MOTOR DRIVE

2.1. POLISHING PRINCIPLE USED FOR THE DEVELOPMENT OF THE PROPOSED SYSTEM

Figure 1 shows a schematic that describes the polishing principle used in this research. Here, abrasive grains (e.g. diamonds) are positioned between the tool and the workpiece, where the tool is made of a soft material (e.g. epoxy resin) and the workpiece is made of a hard material (e.g. cemented carbide).

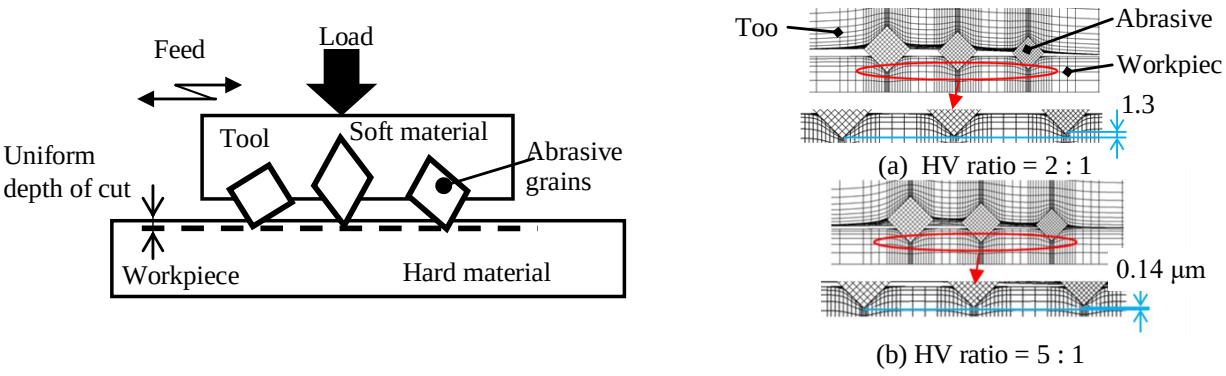

Fig. 1. Schematic views of the polishing principle and FEM simulations at different Vickers hardness ratios

The tool is then subjected to a load to be in contact with the workpiece, which causes the abrasive grains between the tool and the workpiece to become embedded to the soft material tool and indent the workpiece. Here, the embedment depth of the abrasive grain

into the tool varies depending on the size and shape of each grain but the indentation depth of the grain into the workpiece is thought to be almost uniform [5, 6]. The tool is then moved in the horizontal direction in an oscillating way under a constant load to scratch the surface with the abrasive grains embedded to the tool. In this regard, a mirror-like finish was defined as a scratch depth of 0.1 μm or less. Moreover, as shown in Fig. 1, as the hardness ratio between the workpiece and the tool increases, the indentation depth into the workpiece tends to become uniform [5, 6]. As observed in previous researches based on FEM software LS-DYNA calculations, it was experimentally confirmed that a mirror-like finish is possible to achieve when the Vickers hardness ratio (HV ratio) becomes 5:1 (where workpiece hardness: tool hardness = 5:1) as a 0.14 μm indentation depth is achieved [6]. From this principle, an automatic mirror-like finish polishing of small flat parts should be possible with a simple and affordable system.

2.2. ACCURACY OF LINEAR MOTOR DRIVE

The selected small linear motor for a high-speed mirror-like finish polishing of small parts was obtained from a Panasonic ES-LV 5B Shaver [7]. Among compact linear motors, the size of the selected unit was observed to be extremely compact, with a simple shape, easy to obtain and affordable. Thus, it was an attractive option for the intended use in a polishing system. In Table 1, the basic specifications of the compact linear motor used in this research are shown. Similarly, the basic specifications of ultrasonic motors used in similar machining researches are also shown [8–13]. These ultrasonic motors present a reciprocating motion that is quite rapid as they span from 28 kHz to 60 kHz, but their amplitude is as small as 2 μm to 7.5 μm. Thus, the average speed is 2352 mm/min to 12600 mm/min. On the other hand, the frequency of the compact linear motor in the shaver [7] used was 0.23 kHz, which is an extremely slow reciprocating motion and a 1/120 of to that of ultrasonic motors. Meanwhile the amplitude is as large as 1000 μm, and the average speed is extremely high at 14000 mm/min. Therefore, the high-speed drive characteristics of this compact linear motor were used in this research. Subsequently, the precision of this compact linear motor drive was measured and evaluated. For this, in Fig. 2 the experimental setup used for measuring the accuracy of the linear motor drive is shown.

Table 1. Comparison chart between linear and ultrasonic motors

Specification	Shaver [1)]	Ultrasonic motor					
		I [2)]	II [3)]	III [4)]	IV [5)]	V [6)]	VI [7)]
Frequency kHz	0.233	35	60	38.4	28	60	39.2
Amplitude μm	1000	2	2	4	7.5	1	1
Average speed mm/min	14000	4200	7200	9216	12600	3600	2352

[1)]: [7], [2)]: [8], [3)]: [9], [4)]: [10],
[5)]: [11], [6)]: [12], [7)]: [13]

This device is meant to analyze the vibration direction of the compact linear motor in the *X*-axis, the depth direction of the vibration in the *Y*-axis, and the vertical direction of the vibration in the *Z*-axis. As a way to evaluate the machining accuracy, the positioning accuracy at both ends of the stroke in the *X*-axis direction and the variation in both *Y* and *Z*-axis directions were measured. It must be noted that Fig. 2 shows the setup for measurements in the *Y*-direction. The compact linear motor motion shadow was projected with a light source and the behavior of the compact linear motor slider was recorded with a high-speed camera. The variation in the *Y* and *Z*-axis directions was measured and evaluated. In the measurement (*X*-direction) of the positioning accuracy at both ends of the stroke, the linear motor was rotated 90˚ from the position shown in figure 2 and the vibration behavior was recorded. Then, the positions at both ends of the stroke were calculated from the displacement variation of each part of the slider. The measurement accuracy of the high-speed camera was 10.25 μm, and the frame rate was 10000 fps.

In Fig. 3, the experimental results of positioning repeatability (*X*-direction) at both ends of the stroke of the compact linear motor are shown.

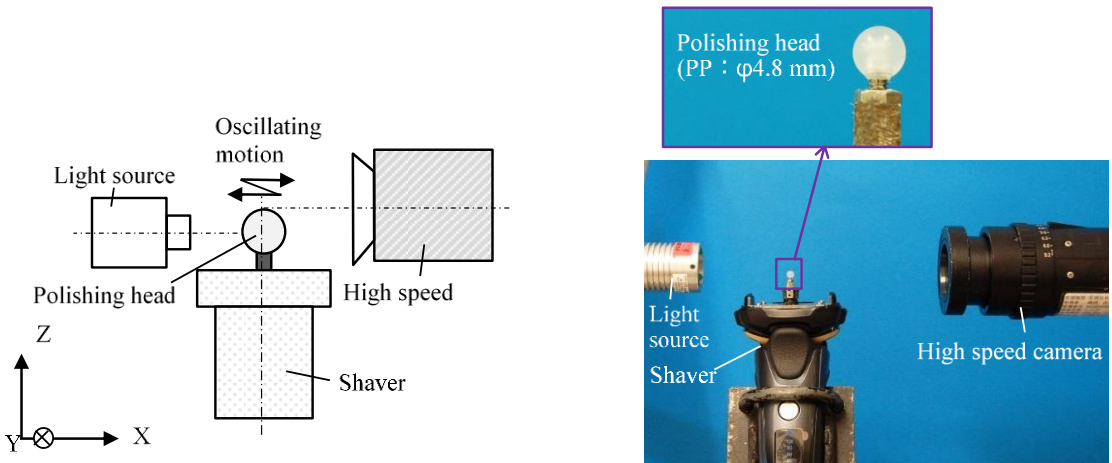

a) Schematic view of the experimental setup b) Photograph of the experimental setup

Fig. 2. Experimental setup used to evaluate the linear motor motion behavior

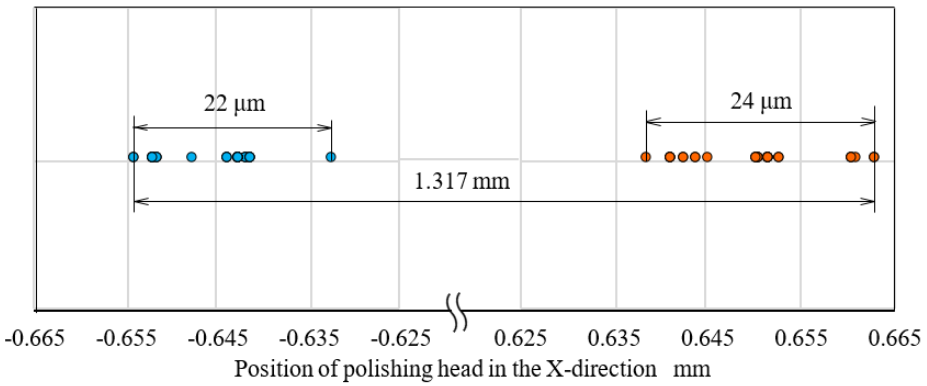

Fig. 3. Measured linear motor positioning accuracy and repeatability in the *X*-direction

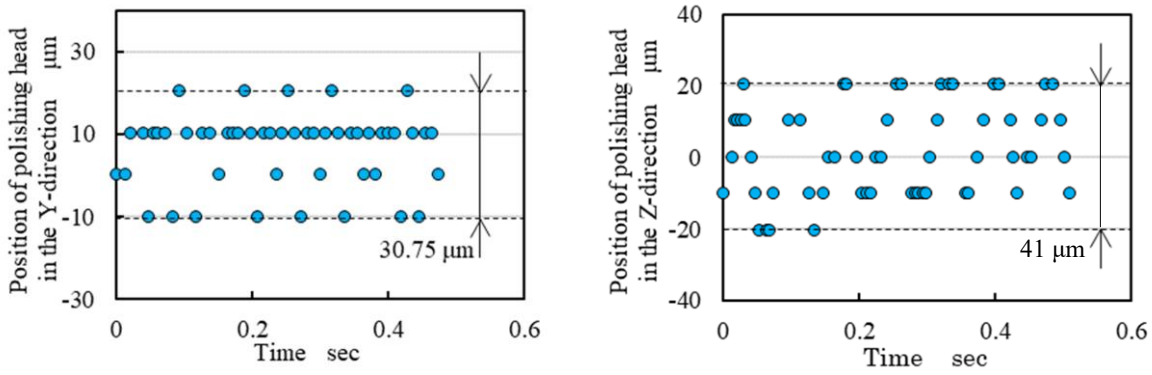

(a) Positioning accuracy in the Y-direction

(b) Positioning accuracy in the Z-direction

Fig. 4. Measured linear motor positioning accuracy in the *Y*- and *Z*-directions

The positioning repeatability of the linear motor strokes were 24 μm on the right and 22 μm on the left side. These results show a reciprocating motion with a repeatability within the range of ± 24 μm for a stroke of 1.317 mm.

Figure 4 shows the experimental results of the variation in the *Y*- and *Z*-axis directions of the compact linear motor. The fluctuation amount of the linear motor in the *Y*-axis direction relative to the initial position is shown. In the range of the stroke (1.317 mm) of the compact linear motor, the maximum variation in the *Y*-axis direction was 30.75 μm. This was considered important factors affecting the dimensional and shape accuracy as well as important for precisely limiting the polishing area of the small parts. Furthermore, the variation in the *Z*-axis of the compact linear motor that affects the machining pressure was measured. The experimental setup used in the previous measurements of the *Y*-axis direction variation and the positioning accuracy (*X*-axis direction) at both ends of the stroke was used for the measurement of the variation in the *Z*-axis. Figure 4 also shows the measurement results for the variation of the *Z*-axis direction relative to the initial position. Within the range of the stroke (1.317 mm) of the compact linear motor, the variation amount was 41 μm. As the polishing head and the workpiece are not in contact via the lapping agent, this behavior does not directly transfer to the workpiece but the variation in the *Z*-axis direction of the polishing head affects the magnitude of the polishing pressure, which in turn affects the indentation depth into the workpiece of abrasive grains in the lapping agent.

2.3. POLISHING PRESSURE OF DEVELOPED POLISHING TOOL

Figure 5 shows a schematic diagram of the polishing tool developed and the apparatus for the measurement of polishing pressure. As shown, a polishing tool was attached to the spindle part of a machine tool. The polishing head used was a commercially available polypropylene ball of Ø4.8 mm with M2×2.5 mm screw hole, which was attached to the slider of the small linear motor via a jig. First, the polishing head was pushed into

an electronic weighing scale using NC control while operating the compact linear motor, and the maximum and minimum loads were measured at that time.

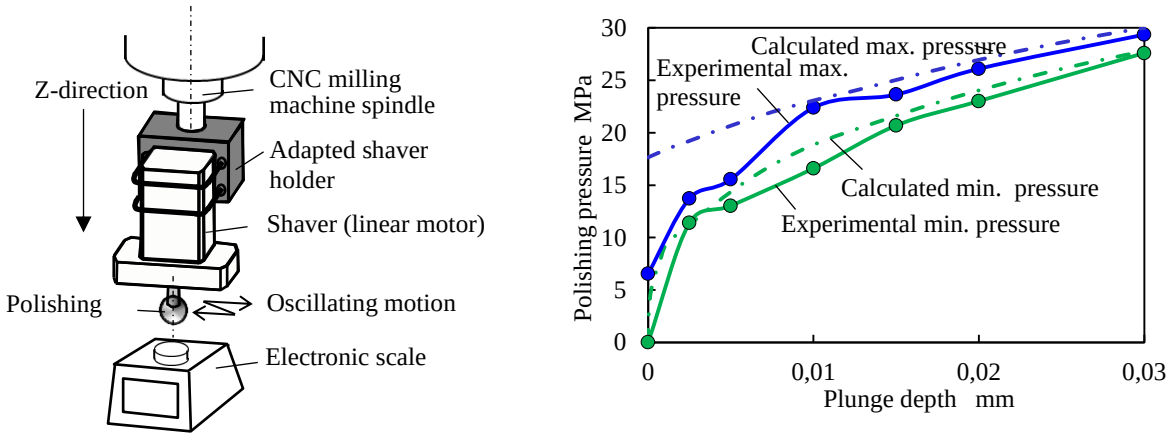

Fig. 5. Schematic view of the experimental setup and the relationship between the plunge depth and polishing pressure

The polishing pressure was calculated from previous measured values and the contact area obtained through the Hertz contact theory. The relationship between the pushing or plunge depth in the *Z*-direction and the polishing pressure is shown in Fig. 5. Furthermore, the polishing pressure calculated from the variation of the polishing head motion in Fig. 4 in the *Z*-direction and Hertz contact theory is also shown. Due to the variation of the small linear motor motion in the *Z*-direction, the polishing pressure fluctuation was about 5 MPa at about a 10 μm depth in the *Z*-direction. As the pressure increased, the variation became smaller. It is expected that this variation affects the improvement of the surface roughness.

2.4. DEVELOPMENT OF LAPPING AGENT AND OPTIMUM PROCESS CONDITIONS DETERMINATION

It is important for the polishing head to hold the captured diamond abrasive grain firmly against the high speed driving of the compact linear motor. Here, when the holding force is insufficient, the abrasive grains are released on the surface of the workpiece upon movement and generate deep indentations which result in a rough surface of the workpiece. Therefore, in the previous section, polypropylene resin with a large holding force was used for the polishing head [6]. PEO-8 (Polyethylene oxide) was added to water uniformly suspend the diamond abrasive grains during the development of the lapping agent [6]. However, there was a concern whether or not the diamond abrasive grains can uniformly float in a stable way when the linear motor is driven at a high speed. At that time, the viscosity of the lapping agent increased due to the addition of PEO, and whether or not diamond abrasive grains are lost during polishing was also a concern. Therefore, it was decided to develop a lapping agent for an improved polishing process through the design of experiments method (DOE). Thus, Fig. 6 shows the experimental method for investigating the optimum machining conditions when using the optimal lapping agent. A carbide V 10 which commonly used for molds was used as the workpiece. The machining

consisted in a repetition motions which were firstly polishing in *Y*-axis direction and secondly polishing for 0.5 mm in *X*-axis direction. Figure 6 also shows the relationship between the processing time and the improvement of the surface roughness when polishing with diamond abrasive grains at a constant grain size.

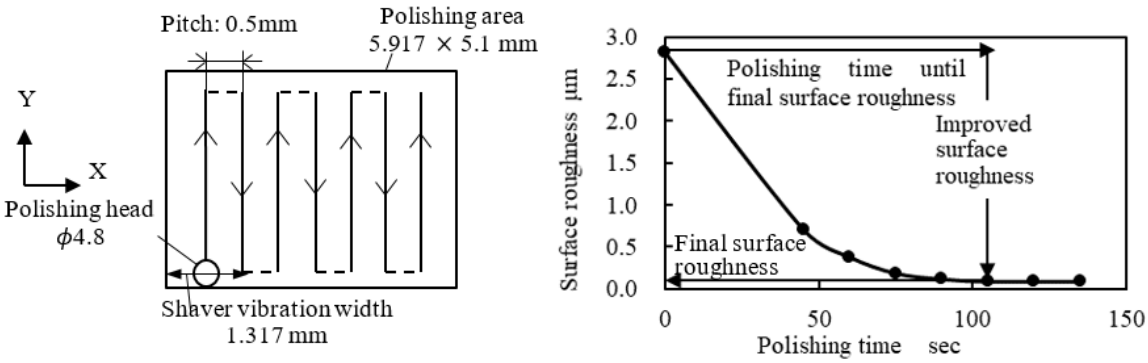

Fig. 6. Machining procedure and the relationship between the surface roughness and the polishing time

A first order lag is observed by this relationship and when it reaches a steady state after a certain machining time a further improvement of the surface roughness is deemed to be not possible (critical surface roughness). The slope of the improvement of the initial surface roughness is defined as the surface roughness improvement rate (= Improvement value of surface roughness ÷ Polishing time to reach critical surface roughness). As the abrasive grain size decreases, both the surface roughness-improving rate and the critical surface roughness become smaller. Table 2 shows the control factors and their levels used in the DOE. Here, the lapping agent consists in diamond, tap water and PEO-8. Based on past experimental results [5], the PEO concentration as the weight ratio of PEO-8 to tap water was set to 0.25 wt%, 0.5 wt%, 1 wt%, 2 wt%, 3 wt% and 4 wt%. The diamond concentration as the weight ratio of diamond to tap water was set to 1 wt%, 2 wt% and 4 wt%. The polishing pressure was set to 5 MPa, 10 MPa and 20 MPa as machining conditions.

Table 2. Parameters used in the orthogonal array to obtain the optimum polishing condition

Control factors	Levels					
	1	2	3	4	5	6
PEO ratio wt%	0.25	0.5	1	2	3	4
Diamond ratio wt%	1	2	4			
Polishing pressure MPa	5	10	20			
Feed speed mm/min	200	700	1500			

The processing feed speed was set to 200 mm/min, 700 mm/min and 1500 mm/min. In order to make the surface roughness of the workpiece *Rz* = 0.1 μm, based on past machining experiments, the following three diamond abrasive grain sizes were used: #400-500, #1200, and #2500 [6]. For each abrasive grain, the surface roughness of improvement rate and the critical surface roughness were examined to determine the optimum lapping

agent and optimum machining conditions. Figure 7 shows a factor effect diagram of surface roughness improvement rate and critical surface roughness obtained from the DOE method. As discussed from Fig. 6, the optimum conditions selection defined for each diamond particle diameter, such as a lapping agent condition and processing conditions, must be selected so that surface roughness improving rate is as high as possible and the critical surface roughness is as small as possible. Machining was performed in ascending order of diamond particle diameter #400–500, #1200, #2500. For diamond grain size # 400–500, PEO concentration of 1 wt%, diamond concentration of 1 wt%, pressure of 20 MPa and feed rate of 1500 mm/min were selected so that the surface roughness improvement rate becomes faster to achieve a productivity improvement in the initial processing stage.

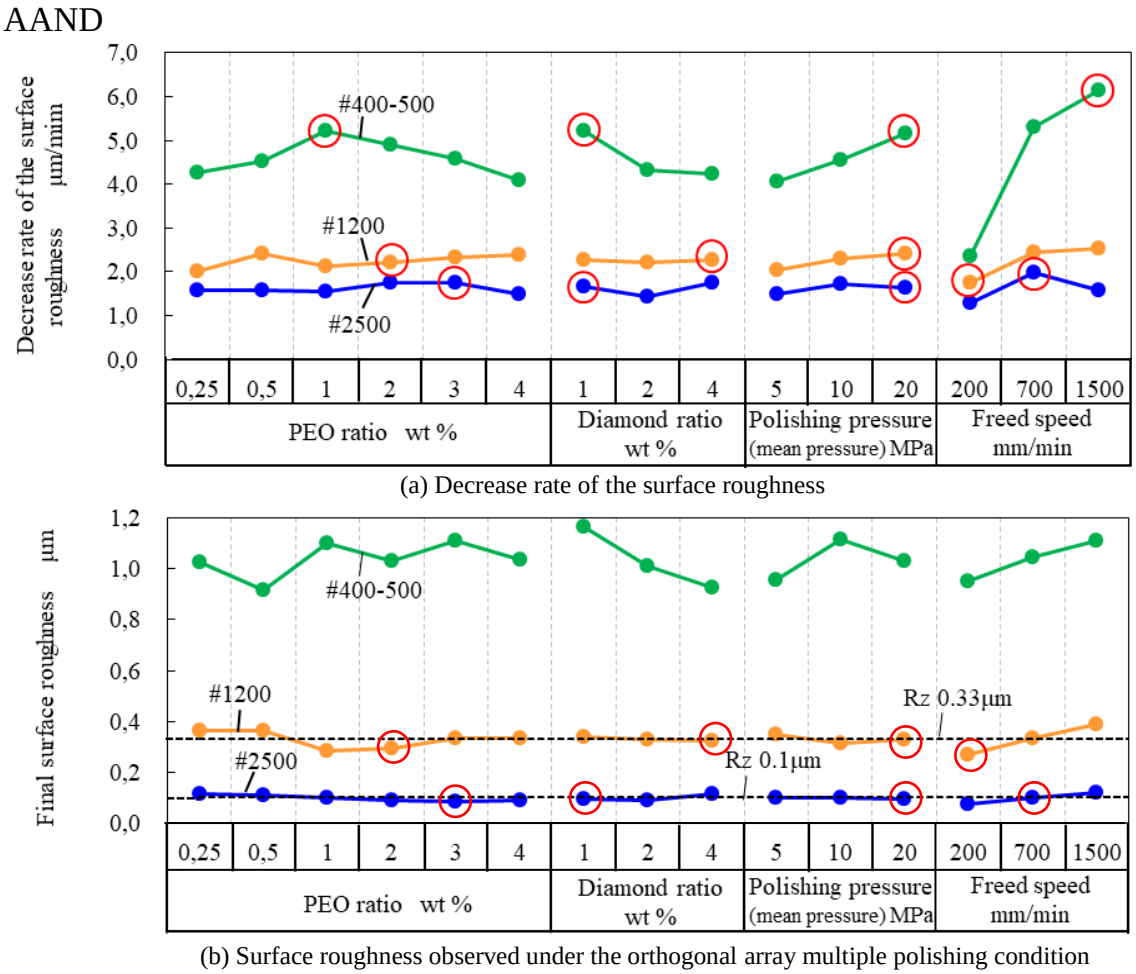

(a) Decrease rate of the surface roughness

(b) Surface roughness observed under the orthogonal array multiple polishing condition

Fig. 7. Factor effect plot from the used orthogonal array

For diamond grain size #1200, both the surface roughness improvement speed and the critical surface roughness were considered at the same time, the processing conditions were set so that the critical surface roughness reached a value lower than Rz = 0.33 μm and the surface roughness improving speed was maximized as much as possible. Therefore, a PEO concentration of 2 wt%, diamond concentration of 4 wt%, pressure of 20 MPa and feed rate of 200 mm/min were selected as machining conditions. For diamond grain size

#2500, since it is the final stage of machining, it is necessary to select the condition that achieves a mirror- like surface. Thus, to achieve a critical surface roughness of less than *Rz* = 0.1 μm, a PEO concentration of 3 wt%, a diamond concentration of 1 wt%, a pressure of 20 MPa and a feed rate of 700 mm/min were selected as processing conditions with high surface roughness improving speed. The red circles in the figure indicates the selected conditions.

Table 3. Lapping slurry specifications

Abrasive grain diameter	Levels			
	PEO ratio wt%	Diamond ratio wt%	Polishing pressure MPa	Feed speed mm/min
#400–500	1	1	20	1500
#1200	2	4	20	200
#2500	3	1	20	700

Table 3 summarizes the selected machining conditions and the conditions of the lapping agent. In the subsequent machining process, it was decided to use the lapping agent shown in Table 3 for each diamond particle size that was used.

2.5. SYSTEMATIZATION USING EXISTING MACHINE TOOLS

Figure 8 shows the developed polishing system and Table 4 shows the specifications of the NC milling machine, polishing tool and lapping agent. The polishing tool attached to the shaving machine was mounted on an existing NC milling machine. The workpiece was fixed to the NC machine table vise and surrounded by a vessel filled with the developed lapping agent. After the linear motor drive is turned on, the workpiece is automatically machined by NC control.

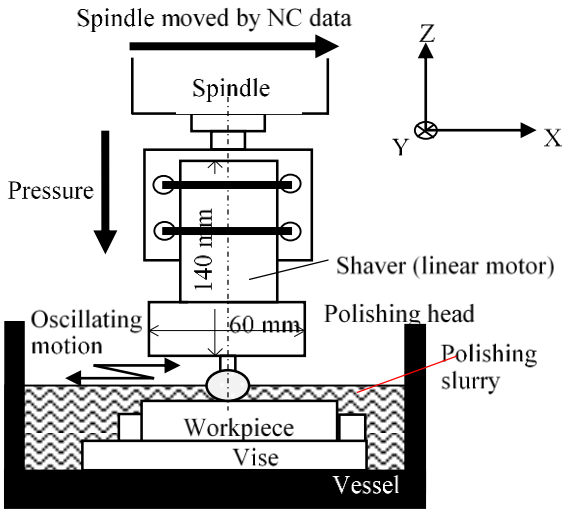

Fig. 8. Schematic view of the polishing experimental setup

The immersion of the workpiece with a lapping agent was designed to withstand a long time automatic lapping operation. Moreover, by using the feed in the *Z*-axis direction of the NC milling machine, the polishing head is able to intermittently catch new diamond abrasive grains (cutting edge). For this reason, when a new abrasive is caught a new cutting edge is formed, which means that the head is refurbished during processing. At the same time, chip removal is also possible during machining.

Table 4. Parameters used in the orthogonal table to obtain the optimum polishing condition

Polishing tool			NC Milling Machine	
Area of polishing head		Ø4.8	Table working surface mm	620×320
Material of polishing head		Polypropylene	Table movement stroke *X*-axis mm *Y*-axis mm *Z*-axis mm	 510 310 385
Frequency	kHz	0.233		
Average speed	mm/min	14000		
Lapping slurry				
Abrasive material		Diamond		
Grain size	#	400-500,1200,2500		
PEO Ratio	wt%	1, 2, 3	Spindle speed min^{-1}	0
Diamond ratio	wt%	1, 4	Feed speed mm/min	200,700,1500

However, in this research, since small parts are subject to polishing, NC milling drive and linear motor drive are superimposed. For example, positioning work was performed with an NC milling machine and high speed polishing was performed with a linear motor. However, when applying pressure in the *Z*-direction, the used shaver fluctuates by 0.209 mm in the *Y*-axis direction due to the swinging mechanism, which affects the dimensional accuracy in the *Y*-axis.

2.6. DIMENSIONAL ACCURACY OF THE HIGH-SPEED POLISHING MACHINE TOOL SYSTEM

In this section, the developed system that consists in a polishing tool mounted on an existing machine tool was manufactured and its dimensional accuracy (see Fig. 10 and Table 7) was evaluated. Figure 9, to the left, shows the processing procedure for evaluation. Three types of machining areas, 1.433 mm × 1.433 mm, 3 mm × 3 mm and 10 mm × 10 mm were used and the parameters were set with or without accuracy corrections. Here, "Without offset" is defined as considering only the amplitude 1.32 mm (*X*-axis direction) of the linear motor, while "With offset" includes corrections in the *X*- and *Y*-axes. Here, the *X*-axis direction gives an offset in consideration of the measurement result of the positioning accuracy of the linear motor and the tool (correction value in the *X*-axis direction of 0.433 mm). Moreover, the offset given in consideration of the variation amount due to the tool head and linear motor swinging (correction in the *Y*-axis of 0.209 mm) was also considered. Finally, a correction value regarding tool size in the *Y*-axis direction was also considered (correction in the *Y*-axis direction of 0.3478 mm).

Table 5 shows feed amounts and pitches of NC control considering the presence or absence of correction for each machined area at both with and without offsets. Processing was carried out ten times under each condition, and the dimensional accuracy was measured with a microscope.

Table 5. Feed and pitch by NC control

Desired size on a side mm		Without offset		With offset	
		Feed mm	Pitch mm	Feed mm	Pitch mm
1.433	*X*-axis	0.433	0.433	0	0
	Y-axis	1.433		1.0852	
3	*X*-axis	2	1	1.567	0.7835
	Y-axis	3		2.6522	
10	*X*-axis	9	1	8.567	1.2239
	Y-axis	10		9.6522	

Figure 9, to the right, shows the measurement result of machining dimensional accuracy. This is a measurement result of the dimensional error at each setting value. For this, when processed under “without offset”, the dimensional error was 0.370 to 0.417 mm in the *X*-axis direction and 0.313 to 0.368 mm in the *Y*-axis direction. On the other hand, under the processing condition “with offset”, the dimensional error was –0.011 to 0.023 mm in the *X*-axis direction and –0.020 to 0.021 mm in the *Y*-axis direction. The minimum processing area of this system was 1.433 ± 0.023 mm × 0.3478 ± 0.021 mm.

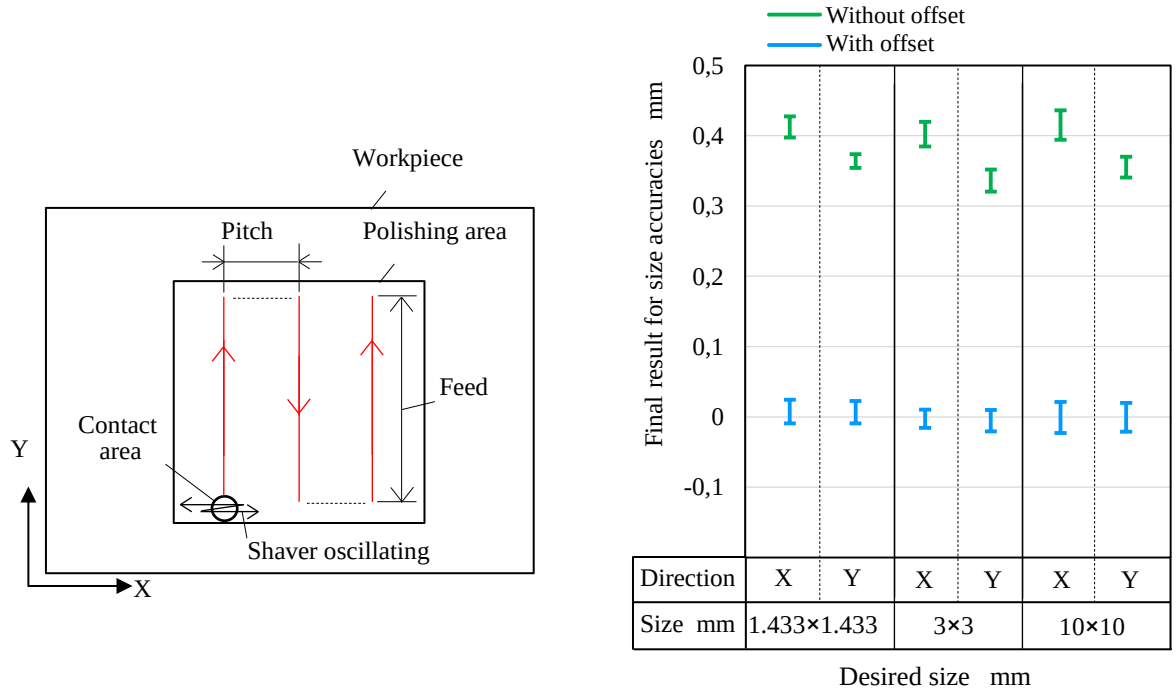

Fig. 9. Polishing pattern and dimensional accuracy results

3. EVALUATION EXPERIMENT

In this section, an evaluation of the developed polishing system is presented. Figure 10 shows a polishing process schematic for evaluation. It presents a square of 3 mm × 3 mm and a circular shape of Ø3 mm which are separated by 5 mm in the *X*-axis direction and the *Y*-axis direction. The workpiece was a carbide V10 commonly used for molds. The processing procedure is shown in the right schematic of Figure 10. The red arrow indicates the program trajectory of the machine tool. For the machining of a square shape, an offset of 0.433 mm in the *X*-axis direction and 0.3478 mm in the *Y*-axis direction was applied and three feeds were made in the *Y*-axis direction while shifting the pitch by 0.7835 mm in the *X*-axis direction. In the case of a circular shape, it was divided into three processing procedures I, II and III. Processes I and II, were carried out considering the minimum polishing area 1.433 × 0.3478 mm, 200 coordinate points passing over half of Ø3 mm are connected by linear interpolation as envelopes and processing was carried out through this envelope. In process III, the workpiece was rotated 90 degrees to process the remaining part (the center part and the envelope of the height 1.433 mm) in the process I and II. The optimum polishing conditions were defined as the conditions presented in the previous chapter and the three diamond particle sizes (#400-500, #1200, #2500) and machining was carried out under these. For the evaluation method, the change over time in the improvement of the surface roughness in the shape of a square and a circle was measured with a laser microscope. Dimensional accuracy was measured with a microscope and the shape accuracy (squareness and roundness) was determined from the distance between the datums, plotting two datums at the target location with a microscope. The dimensional accuracy of the shapes was also measured with a microscope. Finally, pictures were taken to confirm the mirror-like surface of the two shapes.

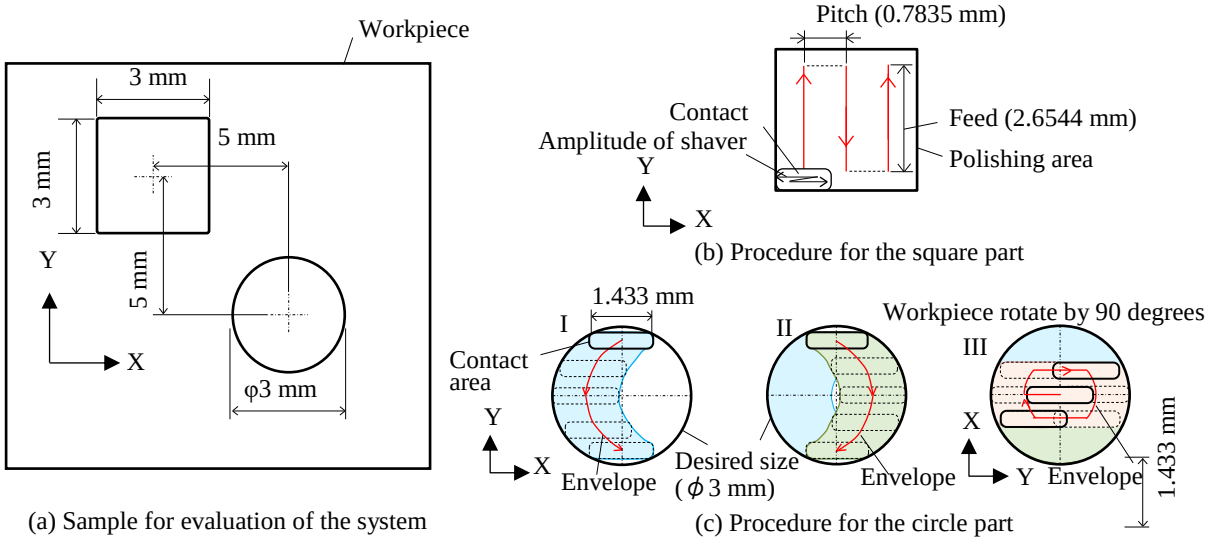

Fig. 10. Schematic of the evaluation sample and the procedure for square and circle parts

Figure 11 shows the measurement results of the change over time in the improvement of the surface roughness of a square shape and a circular shape. Both shapes were deemed as mirror-like surfaces because the surface roughness reached a *Rz* of 0.1 μm or less. The polishing time presented in Fig. 11 does not include setup time such as polishing head exchange, exchange of lapping agent and workpiece cleaning. The polishing time was 33.3 sec for a square shape and 35.1 sec for a circular shape, respectively. Table 6 shows the comparison with ultrasonic polishing (ex. amplitude 2 μm, frequency 60 kHz [9]). If a conversion into the same machining are is done, the proposed system could process the same area in only about 1/2 of the processing time of ultrasonic polishing.

Furthermore, Table 7 shows measurement results of processing accuracy. These are dimensional accuracy, shape accuracy as well as the dimensional accuracy between twoshapes that correspond to the schematic in Fig. 12. For dimensional accuracy, the length ofthe side of the square was +0.016 mm to +0.021 mm, and the diameter of the circular feature had an error of +0.046 mm from –0.115 mm. The shape accuracy was a square perpendicularity of 0.013 to 0.018 mm and a circular roundness of 0.070 mm. This is the result of superimposing the driving of the small linear motor slider, driving error of the NC milling machine, and the precision of the polishing head through a programming method.

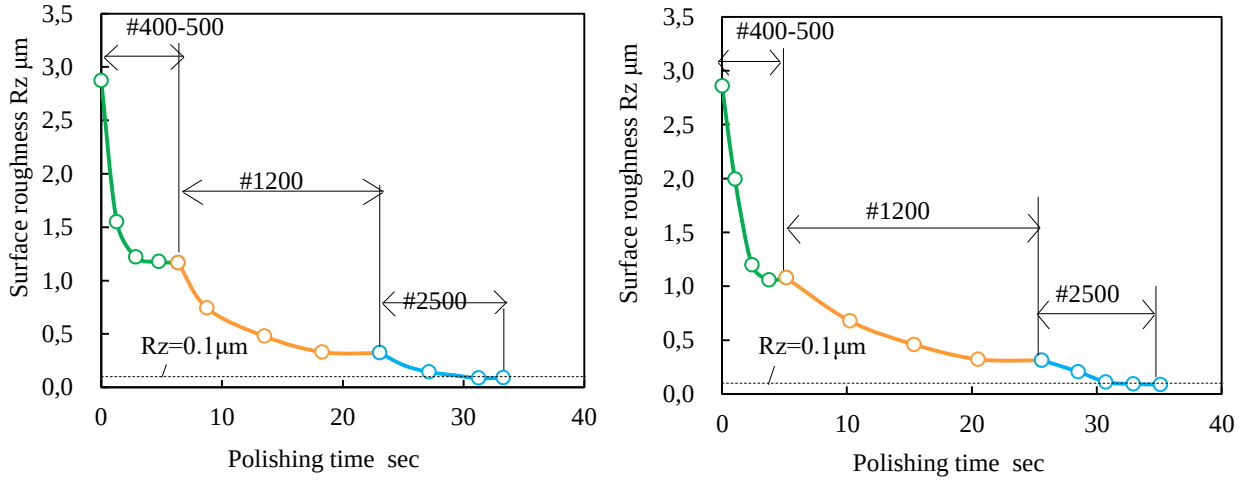

(a) Square (b) Circle

Fig. 11. Relationship between surface roughness and polishing time

Table 6. Comparison chart between proposed system and ultrasonic motors

	Square			Circle		
	Size	Polishing time sec	Time / area sec / mm^2	Size	Polishing time sec	Time / area sec / mm^2
Proposed system (Linear motor)	3 mm × 3 mm	33.3	3.7	Ø3 mm	35.1	4.96
Ultrasonic motor [1)]	10 mm × 10 mm	720	7.2			

[1)] : [9]

Table 7. Processing accuracy results

Square		
Xs		3.016 mm
Ys		3.021 mm
Squareness	A⊥B	0.018 mm
	A⊥C	0.013 mm
Circle		
Diameter-max		3.026 mm
Diameter-min		2.885 mm
Circularity		0.070 mm
Distance between square and circle		
X-dimension		5.01 mm
Y-dimension		5.05 mm

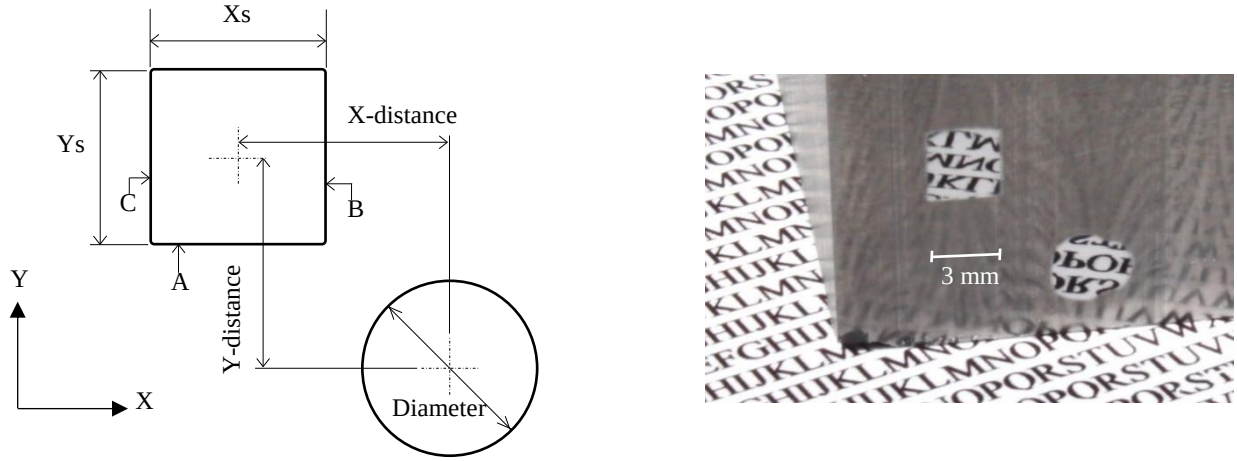

Fig. 12. Polishing accuracy regarding the machined sharpes and a photograph of achieved mirror like

The dimensional accuracy between the two shapes was +0.010 mm in the *X*-axis direction and +0.050 mm in the *Y*-axis direction. It is considered that this is mainly due to the driving error of the NC milling machine. Figure 12 shows the results of photographing the two types of reflection / mirror-like surface state. Here, the appearance of the processed surface was uniform and deemed as a mirror-like surface.

4. CONCLUSIONS

1. The usage of a shaving machine as a compact linear motor drive, a high-speed mirror polishing processing system and processing technology was proposed and constructed as an affordable alternative for high quality, high dignity, simple and cheaply manufacturing.

2. High-speed polishing machining in the range of several millimeters (1.433 mm minimum) was shown as possible.
3. Mirror surface processing with *Rz* of 0.1 μm or less was achieved.
4. Dimensional accuracy of the proposed polishing system for square shapes was an error in the side length between +0.016 mm and +0.021 mm, and for circular shapes an error in diameter between –0.115 mm and +0.046 mm. The shape accuracy was a square perpendicularity error of 0.013 to 0.018 mm and a circular out-of-roundness of 0.070 mm.

REFERENCES

[1] MIZUNO T., 2001, *Spread of machine tool driven linear motors*, The Journal of the Institute of Electrical Engineers of Japan, 121/9, 620–623, (in Japanese).
[2] KARITA M., 1995, *High performance technology in linear motor*, Journal of Japan Society for Precision Engineering, 61/3, 347–350, (in Japanese).
[3] SASAKI T., MIYOSHI T., SAITO K., KATO O., 1991, *Knowledge acquisition and automation of polishing operations for injection mold. (1st report). Hand polishing properties of a skilled machinist*, The Japan Society for Precision Engineering, 57/3, 497–503, (in Japanese).
[4] NAKAJIMA N., 2005, *Micro-Precision machining technology by 3-D surface machining EDMs*, The Japan Society for Precision Engineering, 71/5, 5575–61, (in Japanese).
[5] IYAMA T., TANABE I., TAKAHASHI T., 2009, *Optimization of lapping slurry in automatic lapping system for dies with cemented carbide and its evaluation*, Transactions of the Japan Society of Mechanical Engineers, Series C, 75/749, 210–215, (in Japanese).
[6] IYAMA T., TANABE I., 2011, *Mirror-Like finishing of soft materials using a polishing tool with controllable hardness by heat softening*, Transactions of the Japan Society of Mechanical Engineers, Series C, 77/775 1154–1160, (in Japanese).
[7] PANASONIC, 2016, *Men's shaver specifications*, <http://panasonic.jp/shaver/p-db/ES-LV52_spec.html> (accessed on 12 October, 2016), (in Japanese).
[8] SUZUKI K., UEMATSU T., IWAI M., MAKIZAKI T., 2000, *Ultrasonic grinding utilizing a stator of an ultrasonic motor*, The Japan Society of Mechanical Engineers, Manufacturing & Machine Tool Conference, 2, 183–184, (in Japanese).
[9] HARA K., ISOBE H., KYUSOJIN A., OKADA M., 2008, *Ultrasonically assisted grinding of die steel using diamond electroplated tools*, The Japan Society for Abrasive Technology, 1, 46–51, (in Japanese).
[10] SUZUKI N., YAN Z., HARITANI M., YANG J., HAMADA S., HINO R., SHAMOTO E., 2007, *Ultraprecision machining of tungsten alloy by applying ultrasonic elliptical vibration cutting*, The Japan Society for Precision Engineering, 73/3, 360–366, (in Japanese).
[11] SOUTOME T., SATO K., 2010, *Study on superposition superfinishing*, (4th report, Smoothing of surface roughness by superposition vibration cutting), Transactions of Japan Society of Mechanical Engineers, 76/767, 1850–1858, (in Japanese).
[12] SUZUKI K., UEMATSU T., MAKIZAKI T., 1999, *Ultrasonic grinding development of the ultrasonic ellipse vibration grinding stone*, Ultrasonic Technology, 11/7, 36–40, (in Japanese).
[13] YAMAMOTO T., TORII A., UEDA A., HANE K., 2001, *Vibration measurement of an ultrasonic motor using stroboscopic phase-shift interferometry*, Bulletin of Aichi Institute of Technology, Part B, 36, 9–14, (in Japanese).